

Case Report

Renal Mast Cell Specific Proteases in the Pathogenesis of Tubulointerstitial Fibrosis: Case Report

Dmitri Atiakshin ^{1,6}, Sergey Morozov ², Vladimir Dlin ², Andrey Kostin ¹, Michael Ignatyuk ¹, Galina Kuzovleva ³, Sergey Baiko ⁴, Igor Buchwalow ^{1,5,*} and Markus Tiemann ⁵

¹ RUDN University, 6 Miklukho-Maklaya St, Moscow, 117198, Russian Federation

² Veltischev Research and Clinical Institute for Pediatrics & Pediatric Surgery of the Pirogov Russian National Research Medical University of the Russian Ministry of Health

³ I.M. Sechenov First Moscow State Medical University (Sechenov University), Moscow, Russia

⁴ Belarusian State Medical University, Minsk, Belarus

⁵ Institute for Hematopathology, Fangdieckstr. 75a, 22547, Hamburg, Germany

⁶ Research Institute of Experimental Biology and Medicine, Burdenko Voronezh State Medical University, Voronezh, Russia

* Correspondence: Igor Buchwalow, Institute for Hematopathology, Fangdieckstr. 75a, 22547 Hamburg, Germany. E-mail: buchwalow@pathologie-hh.de. Tel.: +49 (040) 70 70 85 317. Fax: +49 (040) 70 70 85 110; (<https://orcid.org/0000-0003-1142-7483>)

Abstract: Kidney fibrosis is a complex polyetiological progressive disease manifesting as an intraorgan proliferation of the connective tissue with the appearance of cicatricial changes. However, pathogenetic mechanisms of renal fibrosis remain poorly understood. The paper highlights features of the protease phenotype and histotopography of mast cells (MCs) found in the kidney, as the key players in extracellular matrix remodeling in nephrofibrosis, detected in a patient diagnosed with "nephrosclerosis with the non-functioning upper pole of the duplex right kidney in the junction of refluxing megaureter of the upper pole of the duplex right kidney". The highest content of MCs was found in the kidney areas with fibrotic changes. MCs were actively involved in the development of inflammatory and fibrotic changes in limited loci of the specific tissue microenvironment of the kidney through targeted secretion of tryptase, chymase, and carboxypeptidase A3 to the vascular endothelium, nephron epithelium, interstitium cells, and components of the intercellular substance. The formation of a profibrotic environment in the kidney interstitium was facilitated by epigenetic effects of tryptase promoting epithelial-mesenchymal transition (EMT) of the nephron epithelium. A selectively increased number and targeted secretory activity of MCs in limited loci of the kidney parenchyma without visible pathological changes evidence a trigger pathogenetic role of specific proteases in the formation of a local microenvironment with a profibrogenic metabolic profile. Thus, MCs are actively involved in the mechanisms of formation and evolution of fibrogenic niches in the kidney; this fact can be used to develop new strategies for therapeutic options of tubulointerstitial fibrosis resulted from chronic kidney injury. Further study of the molecular phenotype of mast cells reveals new fundamental mechanisms of fibrosis pathogenesis being a significant tool for personalized therapy in nephrology.

Keywords: mast cells; tryptase; carboxypeptidase A3; chymase; fibrogenic niche; kidney fibrosis; specific tissue microenvironment

1. Introduction

Chronic kidney disease is detected in 8-15% of the world's population and leads to a gradual deterioration in organ functioning up to complete loss [1]. Currently, approximately 800 million people represent certain signs of chronic kidney disease, and as estimated, this condition will increase in the foreseeable future [2]. Renal fibrosis, characterized by increased scarring accumulation in the

parenchyma, is a common terminal pathway for chronic and progressive nephropathy. Renal fibrosis affects half of adults over 70 and 10% of the world's population. Therefore, active study of the pathogenesis and protective measures of kidney fibrosis is crucial to improve the prognosis of kidney disease. In recent decades, serious fundamental research studies of the mechanisms of renal fibrosis have been carried out to develop effective therapeutic algorithms. However, it should be noted that until now, numerous issues of the pathobiology of renal fibrosis, preventive measures, algorithms for diagnosis and therapy remain unsolved, the fact requiring constant research into the mechanisms of interstitium remodeling [3,4].

A profibrotic phenotype developing in certain loci of a specific tissue microenvironment is supported by a number of mechanisms that provide persistent changes in pathogenetically important constants of the integrative-buffer metabolic environment. This results in the formation of intraorgan tissue niches with features of the functional architecture of the immune and stromal landscapes selectively accumulating a wide range of pro-inflammatory factors, namely, extracellular vesicles, metabolites, cytokines, chemokines, and growth factors, including those in the kidneys [4-6]. The fibrogenic specific tissue microenvironment has a pronounced inductance and long-term autonomy to stimulate fibroblast proliferation, nephron epithelial damage, microvasculature endothelial alteration, macrophage polarization, and other changes [4,7,8]. Research into the mechanisms of formation of a profibrogenic metabolic environment within the local tissue microenvironment significantly contributes to our understanding of the pathogenetic mechanisms of kidney fibrosis [4,9].

As known, mast cells are crucial regulatory elements of a specific tissue microenvironment with a unique potential in the implementation of innate and acquired immunity, and extracellular matrix remodeling [10-12]. Possessing a wide-ranging repertoire of the receptor apparatus and secretory products, MCs are involved in maintaining both the canonical physiological parameters of local homeostasis and initiating the processes of oncogenesis, allergies, inflammation, fibrosis, and many more [13-15]. The well-known fact of an increased number of intraorganic MCs in loci with fibrotic changes, including the kidneys, has not yet been provided with specific details of their integration into the pathogenetic links of the disease [16-18]. In this regard, further studies are needed to explore mechanisms of MC participation in extracellular matrix remodeling and developing excessive fibrous structures in renal fibrosis. In this study, we focused on the state of specific kidney mast cell proteases (tryptase, chymase, carboxypeptidase A3) in the pathogenesis of tubulointerstitial fibrosis in a patient diagnosed with nephrosclerosis with the non-functioning upper pole of the duplex right kidney in the junction of refluxing megaureter of the upper pole of the duplex right kidney.

2. Results

The fibrous-modified areas of the kidney contained the highest number of MCs, it was calculated both per mm² and the relative total number of cells in the tissue (Table 1, Figure 1). In all zones of the kidney, tryptase-positive MCs had the greatest number (Table 1, Figure 2). The number of CPA3-positive MCs was lower (Table 1, Figure 3), though, in the renal medulla, their relative number was comparable to tryptase-positive MCs. Chymase-positive MCs had the least representation (Table 1, Figure 4), practically lacking in the cortical and medullary areas of the kidney. However, it should be noted that in fibrous foci of the kidney, the content of chymase-positive MCs was significantly higher, especially when determining the relative content among all cells of the fibrous tissue (Table 1, Figure 4a).

Table 1. The content of MCs in the kidney under fibrosis.

Parameters		Tryptase+	CPA3+	Chymase+
Cortex of the kidney	Total number of cells in the analysed area	467240	408847	467609
	Absolute number of MCs in the analysed area	757	347	49

Medulla of the kidney	Relative amount of MCs in the analysed area (B %)	0.16	0.09	0.01
	The content of MCs / mm ²	9.71	5.58	0.39
	Total number of cells in the analysed area	193548	195731	199893
	Absolute number of MCs in the analysed area	214	196	20
	Relative amount of MCs in the analysed area (B %)	0.11	0.1	0.01
	The content of MCs / mm ²	7.36	5.98	0.81
	Total number of cells in the analysed area	274095	251490	188943
	Absolute number of MCs in the analysed area	1617	1080	454
	Relative amount of MCs in the analysed area (B %)	0.59	0.43	0.24
	The content of MCs / mm ²	46.31	27.52	15.26
Fibrous-modified areas of the kidney				

Despite the fact that the relative number of mast cells in the fibrosis-modified area was comparatively low compared to the entire amount of other cells (Table 1), the high secretory activity of MCs attracts attention. In that context, in the kidney there were detected areas (zones) abundantly infiltrated with secretory granules or having tryptase immunopositivity (Figures 1, 2 and 5). The high content of secretory granules with autonomous activity potential and gradual release of biologically active substances, including tryptase, chymase, and CPA3, could significantly enhance the biological role of MCs in individual loci of a specific tissue microenvironment.

MCs forming protease-positive fields with unique inductive properties due to specific protease accumulation was previously described in our studies related to other pathologies (Figures 2 and 5) [22,23].

In terms of cytotopography, specific proteases in certain MCs were packaged into secretory granules of various sizes, in which they occupied a peripheral position (Figure 5). Such intragranular localization of specific proteases was also typical of MCs located in other organs [22-24]. Notably, quite often tryptase, chymase and carboxypeptidase A3 were detected as progranules, small immunopositive formations distributed throughout the cytoplasm. This evidenced active processes of biogenesis, in which synthesis and post-translational rearrangements are accompanied by rapid secretion (Figures 3 and 4). In addition, it is necessary to pay attention to the regulatory potential of MCs, provided by tunneling nanotubes, which are clearly visible in certain loci of the specific tissue microenvironment of the kidney (Figure 5). Occasionally it was possible to observe formation of elongated cytoplasmic outgrowths containing specific proteases directed to target cells (Figure 5). Postcellular structures were often found in fibrotic-modified areas of the kidneys; they were autonomous fragments of the cytoplasm or freely located granules able to secrete biologically active substances for a certain time after separation from the maternal cytoplasm.

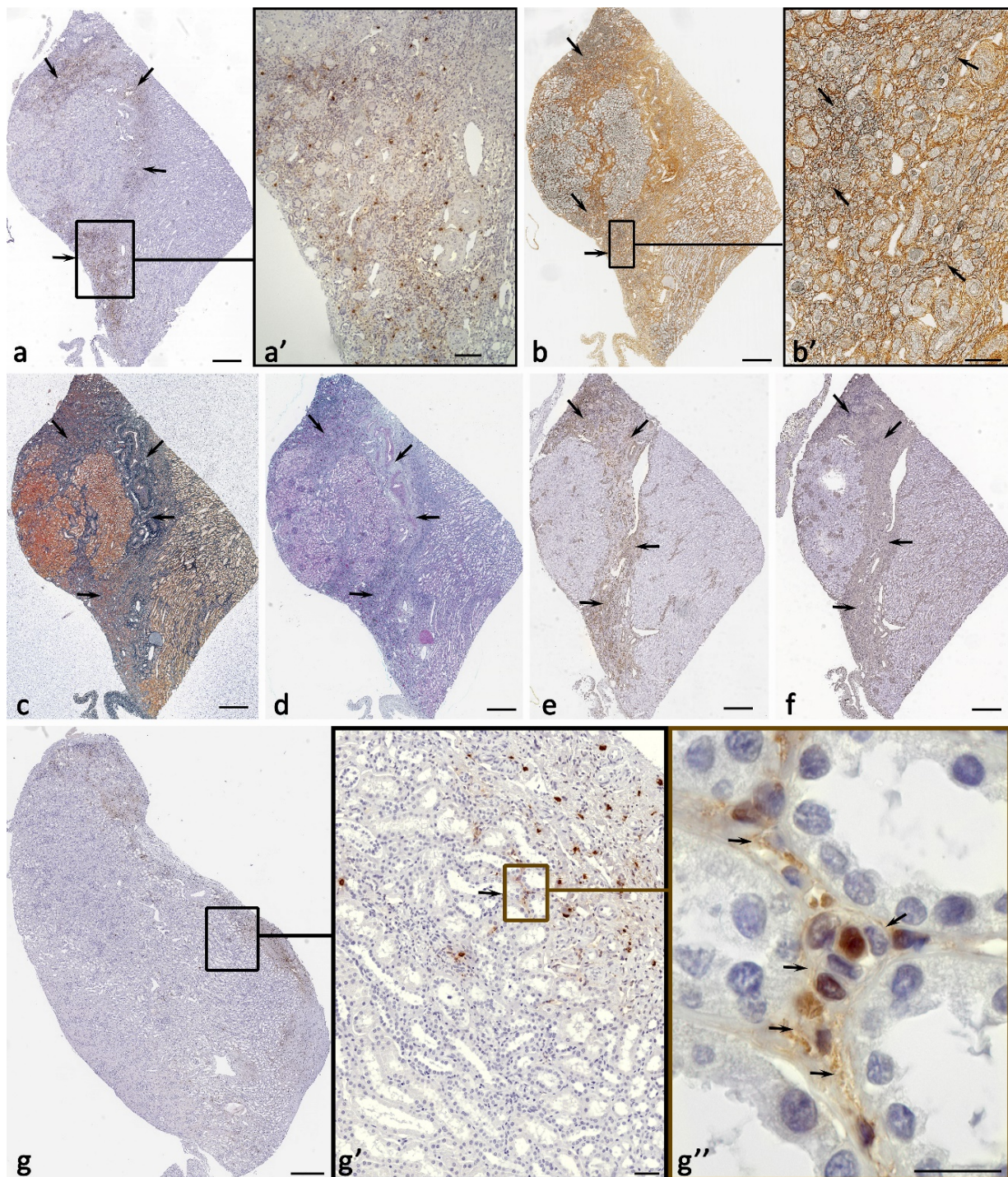


Figure 1. Features of the MC association with elements of the kidney stroma in nephrofibrosis. Technique: **a, e-g** immunohistochemical staining of MC tryptase (**a,g**), α -SMA (**e**) and vimentin (**f**); **b** silver impregnation; **c** Heidenhain azan staining; **d** alcian blue staining and PAS staining. **a** Selective localization of tryptase-positive mast cells in the kidney with high protease secretion activity (arrowed). **a'** Enlarged fragment **a**. **b-d** Formation of distinct tryptase-positive inductive fields, coinciding in localization with areas of high content of reticular fibers and collagen fibrillogenesis (**b, b'**, arrowed), as well as collagen fibers and an amorphous component of the extracellular matrix of the connective tissue (**c, d**, arrowed). **e, f** Colocalization of intraorganic expression of α -SMA (**e**) and vimentin (**f**) with mast cell histotopography (arrowed). **g** Participation of mast cells in the formation of a profibrogenic niche with a tryptase-inductive zone in the unaltered kidney parenchyma (**g'**, arrowed) (**g''**, arrowed). Scale: **a', b', g'** – 50 μ m, **g''** – 5 μ m, the rest – 500 μ m.

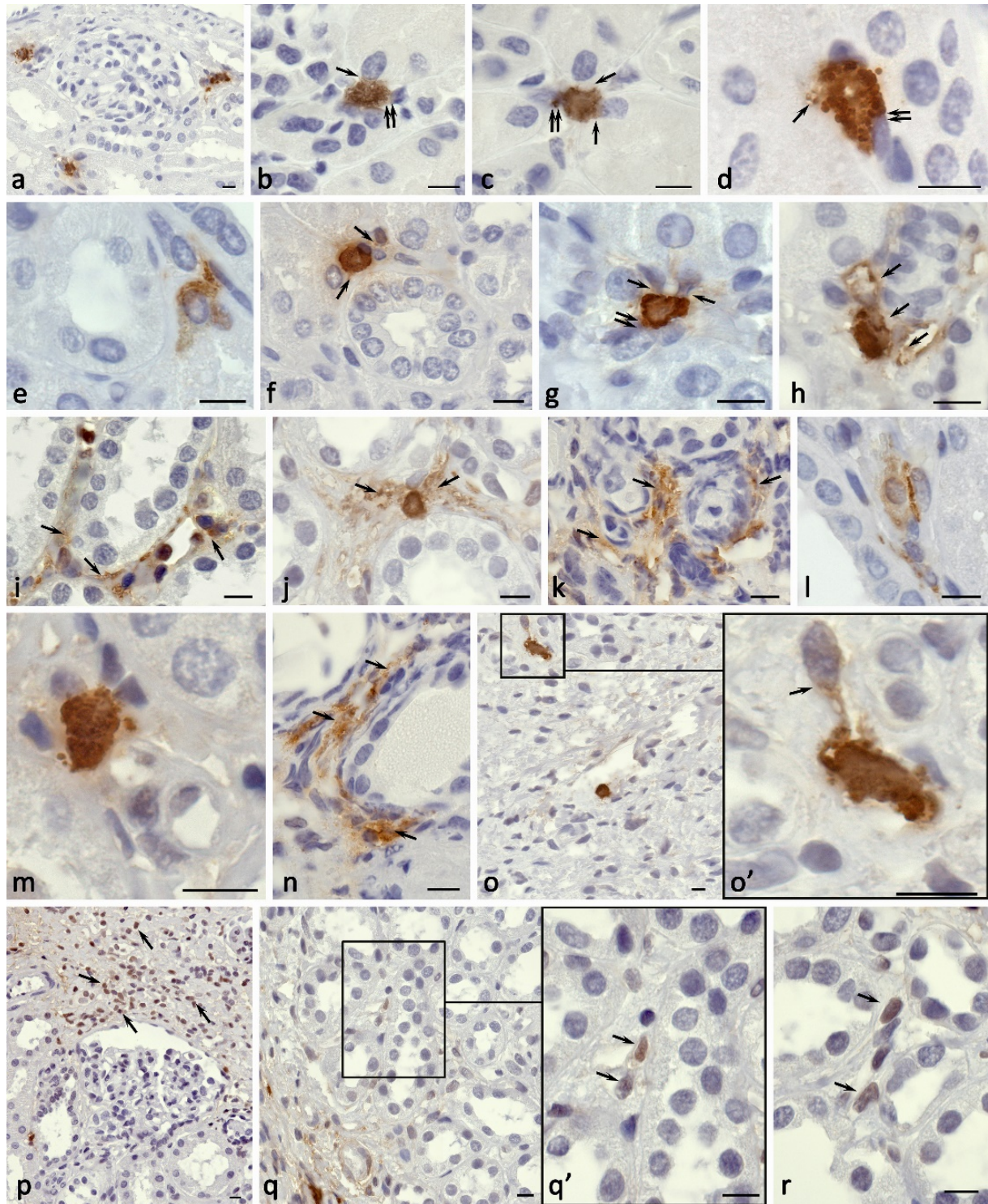


Figure 2. Histo- and cytotopography of mast cell tryptase under the formation of fibrotic changes in the kidney. **a** Close mast cell localization to the renal corpuscle in the cortex. **b-d** Target tryptase secretion by mast cells to the basement epithelial membrane of the proximal convoluted tubule of the nephron (arrowed) and interstitium cells (double arrowed). **e** Tryptase secretion to the basement membrane of the epithelium of the distal convoluted tubule of the nephron and to the structures of the interstitium (arrowed). **f** Tryptase secretion into the extracellular matrix of the kidney interstitium in the cortex at the border of the distal and proximal convoluted tubules of the nephron (arrowed). **g** Interaction of mast cells with stromal cells in the renal cortex (arrowed), including fibroblast (double arrowed). **h-n** Options for the formation of profibrogenic niches by mast cells in the interstitium of the kidney with local tryptase accumulation in the extracellular matrix (arrowed). **o** Target tryptase

secretion to the stromal cell with penetration into the nuclear structures (arrowed). **p-r** Tryptase-positive nuclei in the cells of a specific tissue microenvironment of profibrogenic renal niches. Positivity of the nucleus to tryptase, mainly in the cells of the interstitium (arrowed) is highlighted. Scale: 10 μ m.

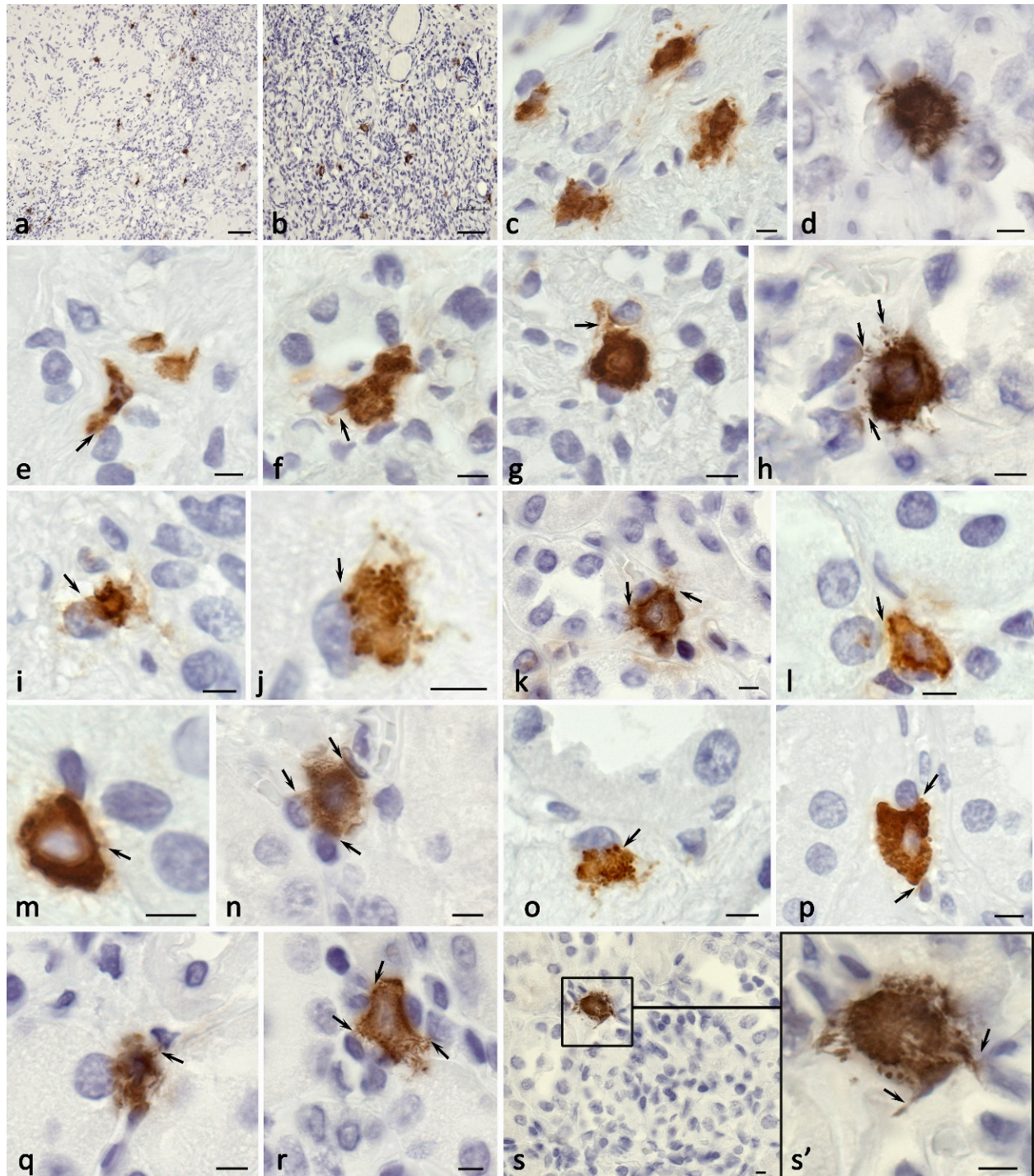


Figure 3. Carboxypeptidase A3-positive mast cells in the kidney in nephrofibrosis. **a, b** High content of mast cells in the kidney area with fibrotic changes. **c** Mast cells form groups in the paracrine zone near the fibroblast (arrowed). **d** Colocalization of mast cells with several stromal cells in the area of fibrosis, active secretion of CPA3. **e-g** Secretion of CPA3 to the epithelium of the nephron (arrowed) in fibrous areas of the renal medulla. **h** Simultaneous effect of CPA3 on the nephron epithelium and interstitium cells (arrowed). **i** Mast cell participation in the epithelial-mesenchymal transformation of nephron cells (presumably; arrowed). **j** MC colocalization with myofibroblast of the interstitium of the kidney (presumably; arrowed). **k-s** Morphological equivalents of MC participation in the

formation of profibrogenic niches with CPA3 secretion (arrowed) to the targets of a specific tissue microenvironment, including the epithelium of the proximal and distal convoluted tubules (**k-m**), interstitium cells (**n-r**) and leaves of the Shumlyansky-Bowman's capsule (**s**). Scale: a, b - 50 μ m, the rest - 5 μ m.

Histotopographic features of the MC distribution in the kidney interstitium allowed revealing the following fact: regardless of the specific protease expression, MCs in the cortical substance were most often located in the region of the proximal or distal convoluted tubules contacting the basement membrane of the nephron epithelium (Figures 1g, 2a-h, 3k-s and 4b-d). Mast cells could be localized near the renal corpuscle, sometimes in contact with the parietal leaf of the Shumlyansky-Bowman's capsule (Figures 2a and 3s). MCs in the medulla were most commonly localized in the interstitium near the loop of Henle (Table 2).

Table 2. Histotopography of MCs in the interstitium of the cortex and medulla of the kidney with fibrosis (in % of the total number of mast cells).

Protease phenotype of MCs	Localization in the renal cortex			Localization in the renal medulla	
	Microenvironment of the capsule of the renal corpuscles	Microenvironment of the proximal convoluted tubules	Microenvironment of the distal convoluted tubules	Collector tubules	the loop of Henle
Tryptase ⁺	22.80	54.90	22.30	34.60	65.40
CPA3 ⁺	11.70	72.20	16.10	11.90	88.10
Chymase ⁺	6.10	43.40	50.50	33.30	66.70

MCs demonstrated active secretory activity of specific proteases in the stroma of the kidney. MCs actively interacted with the parietal leaf of the Shumlyansky-Bowman's capsule (Figure 3s), proximal convoluted tubules (Figures 2b-d,g-h, 3k-m,q-r and 4b-c), distal convoluted tubules and the loop of Henle (Figures 2j,m, 3k,o and 4d). In the sclerosis zone, active MC interaction with other immunocompetent cells and, apparently, with stromal cells was noted (Figures 2b-d,g,m,o, 3c-d,g-j,n-r, and 4a,d-j,l-n). MC interaction with other cells of the local tissue microenvironment was not accompanied by the classical pathways of mediator degranulation solely, but also by forming tunneling nanotubes, which served as an effective way of targeted delivery of specific proteases to cellular targets (Figure 5).

MC migration into the intertubular matrix and, in some cases, protease secretion directly to the basement epithelial membrane of various parts of the nephron caused an obvious loss of contacts between the epithelium and the basement membrane. These evidences can be associated with the phenomena of epithelial-mesenchymal transition, in which the cellular functional potential changes significantly developing a pronounced ability to synthesize extracellular matrix components. Notably, there were tryptase-positive areas formed in isolated loci of the tissue microenvironment; they had a pronounced immunopositivity to the protease and inductance in relation to the development of inflammation (Figures 1a,g and 2h-n).

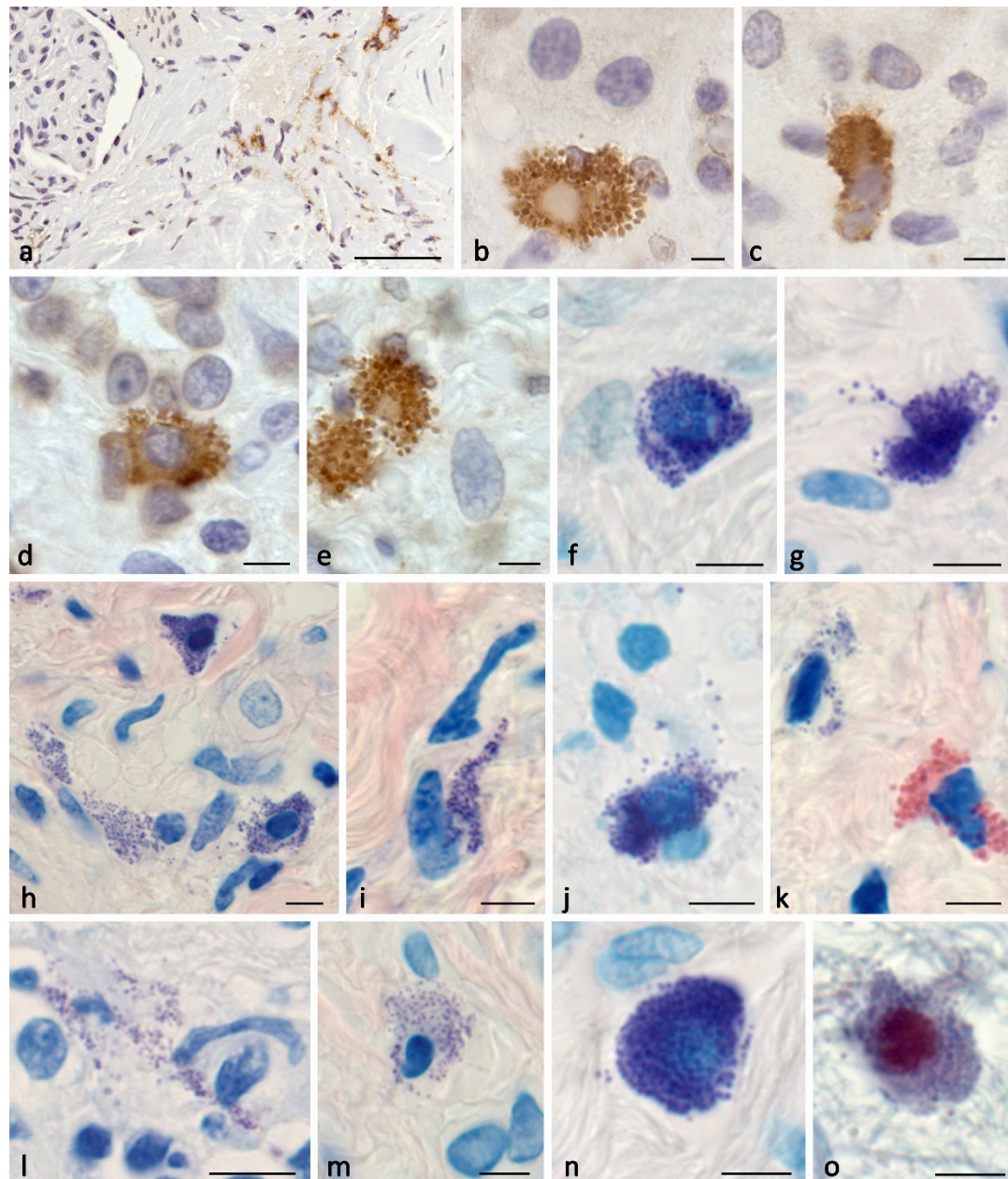


Figure 4. Mast cells in the formation of profibrotic changes in the kidney. Techniques: **a-e** Immunohistochemical staining of mast cell chymase; **f, g, k-n** Staining with toluidine blue; **h-j** Giemsa staining; **o** Picro-Mallory staining. **a** Accumulation of chymase in mature fibrous tissue (arrowed) at the border with the renal cortex. **b-e** Target chymase secretion to the basement membrane of the epithelium of the proximal (**b, c**, arrowed), distal (**d**, arrowed) parts of the kidney nephron. **e-h** Directed mast cell degranulation to fibroblasts in the zone of fibrotic changes (arrowed). **i** Mast cells at the periphery of a profibrogenic niche with active secretory activity (arrowed). **j** Colocalization of mast cell and eosinophil in fibrous tissue. **k-n** Various variants of mast cell secretory activity through autonomous secretory granule excretion into the extracellular matrix (arrowed), resulting in a decreased number of granules in the cytoplasm (**l**) and the formation of areas of a specific tissue microenvironment filled with secretory granules (**m**). **n-o** Variants of MC colocalization with a fibrous component of the extracellular matrix in the kidney area with fibrotic changes. Scale: **a** - 50 μm , the rest - 5 μm .

When determining α -SMA and vimentin expression in various areas of the kidney, it was found that the highest values of the cell and structure immunopositivity were detected in the zone of fibrosis (Table 3, Figures 1e,f). Concurrently, the values of the content of smooth muscle actin and vimentin correlated with each other, the fact supporting an increased representation of mesenchymal

structures due to a potential intensification of the epithelial-mesenchymal transformation of the kidney parenchyma. Much lower values of the content of α -SMA- and vimentin-positive structures were obtained in the cortical and medulla of the kidney (Table 3, Figures 1e,f).

Table 3. The content of α -SMA- and vimentin-positive cells and structures in the kidney.

Kidney areas	Vimentin				a-SMA			
	Immuno-negative structures		Immuno-positive structures		Immuno-negative structures		Immuno-positive structures	
	%	the area (mm ²)	%	the area (mm ²)	%	the area (mm ²)	%	the area (mm ²)
The zone of fibrosis	45.8	2.43	54.2	2.83	45.5	2.15	54.5	2.83
The cortical of the kidney	77.6	8.83	22.4	2.63	86.2	9.47	13.8	1.37
The medulla of the kidney	63.2	5.37	36.8	3.07	89.1	7.84	10.9	0.93

MCs seem to initiate primary changes in the kidney stroma at the sites of subsequent inflammatory process and fibrosis development, in fact creating conditions for the formation of a profibrogenic niche (Figure 1g). A limited zone with a greater number of tryptase-positive nuclei was detected at the border of the unaltered kidney parenchyma contacting with the fibrous tissue (Figure 2p). In the loci of profibrogenic niches, tryptase-positive nuclei were presented; these being combined with the almost completely lacking tryptase expression in the cell nuclei in both the parenchyma and the interstitium of the cortical and medulla of the kidney (Figures 1g, 2o-r). The epigenetic effects of tryptase were involved in creating the profibrotic phenotype of a specific tissue microenvironment by reprogramming and modifying the functional activity of other cells, leading to further progression of fibrotic changes (Figure 2o). The frequency of tryptase-containing nuclei in kidney cells was the highest in the areas with fibrotic changes, or the border areas of the normal parenchyma with pathologically altered areas. Planimetric analysis evidenced a significantly excessive number of cell nuclei with tryptase immunopositivity in fibrous foci of the kidney compared with similar parameters in the cortical and medulla, reaching differences in 10 or more times (Table 4).

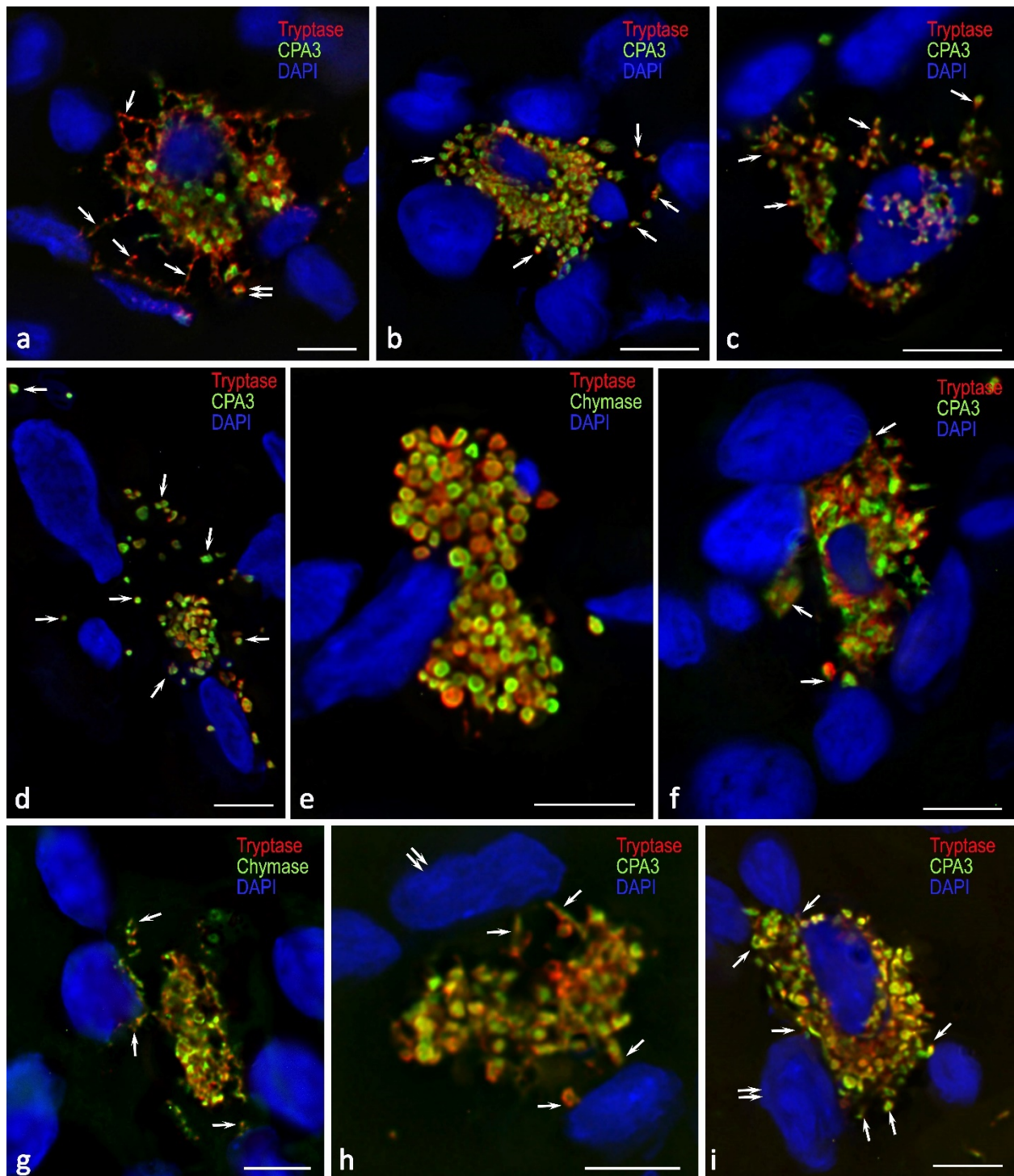


Figure 5. Profile of specific mast cell proteases during the formation of profibrogenic niches in the kidney stroma. **a** Active entry of tryptase and CPA3 to the targets of the extracellular matrix of the specific tissue microenvironment of the tissue niche in the composition of tunneling nanotubules (arrowed) and secretory granules (double arrowed). **b** Entry of tryptase and CPA3 into the profibrogenic niche as part of secretory granules (arrowed). **c-d** Dissemination of secretory granules with specific mast cell proteases in the interstitium (arrowed) adjacent to the stroma cells. **e** Contacting areas of the mast cell cytoplasm filled with large secretory granules, with predominant localization of tryptase and chymase along the periphery of the granules. **f, g** Mast cells in the state of secretion of specific proteases to the epitheliocytes of the nephron tubules (arrowed) of the renal medulla. **h, i** Active secretion of tryptase and CPA3 to interstitial cells of the fibrous part of the kidney (arrowed), including fibroblasts (presumably; double arrowed).

Mast cells were often colocalized with cells expressing smooth muscle actin. Such cells could be both smooth myocytes in the wall of the vascular bed of the kidney and myofibroblasts, since their number increased in the areas with fibrotic changes.

Table 4. Tryptase expression in the cell nuclei of various kidney areas.

Immunopositivity of nuclear structures to tryptase	The cortical % of the total number of nuclei	The medulla % of the total number of nuclei	The zone of fibrosis % of the total number of nuclei
Moderate (+)	0.0225	0.0250	0.3425
Pronounced (++)	0.0073	0.0055	0.1025

Epifluorescence and confocal microscopy findings allowed evaluating spatial orientation of the mast cell secretome effect, in particular, tryptase and carboxypeptidase A3, on the structural components of the epithelium in various parts of the nephron. As appeared, the secretion of protease-containing components could occur on a fairly large area of the basement membrane in both the proximal and distal convoluted tubules of the nephron. There is no doubt that this effect of specific proteases was accompanied by significant changes in the activity of the nephron epithelium. On the other hand, it was found that mast cells were able to simultaneously influence on several targets of the local tissue microenvironment, actually synchronizing the induced changes in the corresponding signaling systems in multiple cells (Figure 5). The formation of a large area of contact between MCs and other cells allowed potentiating biological effects of tryptase, carboxypeptidase A3, and chymase (Figures 5a,b,f). As a rule, in the area of fibrosis, mast cells had a simultaneous effect on a greater number of other cells of the local tissue microenvironment compared to the cortex or medulla of the kidney. In some cases, a mast cell was able to directly secrete proteases simultaneously to eight or more cells depending on the thickness of the histological section (Figure 5).

3. Discussion

In terms of pathobiology, fibrosis is viewed as a protective body reaction aimed at isolating the focus of inflammation from the surrounding tissues and systemic blood flow. Fibrous tissue replacement results in a gradual loss of their specific functions when a certain extent of the integral dysfunction of the organ is reached. The reasons for such changes can be radiation, trauma, infectious-allergic, autoimmune and inflammatory processes. Damage to the kidney can provide a special status of the integrative-buffer metabolic environment of the tissue microenvironment, which undergoes dynamic changes in its composition and content under regeneration and remodeling of the extracellular matrix and spatial architectonics of the organ. To structurally specify these changes in the tissue microenvironment, the term “fibrogenic niche promoting fibroblast activation and myofibroblast formation in organ fibrosis” was previously appropriately proposed [25]. One of the mechanisms for fibrosis formation is epithelial-mesenchymal transition, in which epithelial cells acquire phenotypic properties of mesenchymal cells. Our study findings involving the kidney of a patient with advanced nephrofibrosis evidence the direct MC involvement in the formation of fibrogenic niches and active contribution to fibrosis through several mechanisms.

First of all, it should be noted that mast cells form a pro-inflammatory profile in the local tissue microenvironment of the kidney with the help of specific proteases. Temporal and spatial patterns of tryptase secretion in the local tissue microenvironment of the kidney during MC activation is the most significant pathogenetic event providing the inflammatory process and further formation of a profibrogenic niche. Notably, chronic MC activation can induce formation of hypersensitivity to a number of components of a specific tissue microenvironment due to restructuring of its proper receptor apparatus, thus provoking a higher secretion of biogenic amines, cytokines, and specific proteases [26-28].

Mast cell tryptase is characterized by high biological activity affecting the state of numerous cellular and non-cellular components of the tissue microenvironment [22,29-31]. Several studies have demonstrated close involvement of tryptase in the processes of angiogenesis [32,33], which is

combined with the connective tissue remodeling, secretion of growth factors, cytokines and chemokines, matrix metalloproteinases (MMP) [34].

Kidney fibrosis is accompanied by an increased content of myofibroblasts, more than a third of them originating from tubular epithelial cells [35,36]. As known, tryptase have effects on the cells of fibroblastic differon causing their active migration, mitotic division, and stimulation of the synthesis of collagen proteins. Thus, tryptase effect may contribute to renal fibrosis. The increased expression of smooth muscle actin demonstrated in our study supports the increased number of myofibroblasts at the sites with fibrotic changes and the high intensity of epithelial-mesenchymal transition under the influence of specific MC proteases.

In addition, tryptase has a high affinity for PAR-2 receptors on various cells of a specific tissue microenvironment potentiating the development of inflammation [34]. A crucial regulatory mechanism of tryptase providing potentiation of inflammation is a persistently increased expression of PAR-2 receptor in target cells [32,37,38].

Chymase is of critical role in signaling molecular-cellular integrative mechanisms of a specific tissue microenvironment [23,31,39]. Chymase is able to promote recruitment of immunocompetent cells from the microvasculature to tissues under various conditions. There is evidence of an increased accumulation of various types of inflammatory cells, including eosinophils, under the action of chymase, the fact that we recorded in our study (Figure 4k) [39-41]. Chymase has a direct effect on the activity of various components of the extracellular matrix, having a greater destructive potential compared to tryptase [34,39,42].

As reported, chymase actively correlates with the progression of inflammatory diseases of various organs, including the kidneys [39,43]. Pro-inflammatory effects of chymase are associated with activation of cytokines and growth factors, including IL-1 β , IL-8, IL-18, TRF- β , endothelin-1 and -2, neutrophil-activating protein-2, etc., which leads to the recruitment of granulocytes, lymphocytes and monocytes into the tissue microenvironment [39]. Chymase is likely to cause degradation of contacts and structures that ensure the strength of attachment of epithelial cells to each other and the basement membrane [44]; this can indirectly contribute to epithelial-mesenchymal transformation.

However, the role of chymase in collagen biogenesis is of particular relevance. On the one hand, chymase induces an increased mitotic activity of fibroblasts along with their biosynthetic potential. On the other hand, chymase is involved in the modification of procollagen molecules, inducing the formation of collagen fibrils [34,45]. The conducted studies evidence active MC participation in the mechanisms of fibrillogenesis, which is manifested by an inductive effect on the formation of the fibrous component of the tissue microenvironment, primarily in the pericellular space of fibroblastic differon cells. The presence of reticular fibers or points of fibrillogenesis initiation was also detected in close proximity to the MC plasmalemma [17].

Despite the abundance of CPA3 in mast cells, there is currently a lack of knowledge about its biological effects compared to other specific mast cell proteases - tryptase and chymase [31,46,47]. The crucial role of CPA3 in the biogenesis of the fibrous component of the extracellular matrix and remodeling of the extracellular matrix is assumed. On the one hand, the CPA3-chymase complex can induce an increased mitotic activity of fibroblasts along with their biosynthetic potential. On the other hand, this complex or proteases solely can participate in the procollagen molecule modification inducing the formation of collagen fibrils [34,45]. Previously, we demonstrated the active MC participation in the mechanisms of fibrillogenesis, which is manifested by an inductive effect on the formation of the fibrous component of the tissue microenvironment, primarily next to the cellular representatives of fibroblastic differon [17].

Post-translational histone modifications result in activation or suppression of target genes due to modulated binding of transcription agents to their respective nuclear promoter elements [48]. Several studies have reported that histone modifications are critical in the development and progression of renal fibrosis [49]. Histone acetylation is regulated by three families of proteins, including histone acetyltransferases (HATs), histone deacetylases (HDACs) and bromodomain and extraterminal (BET) proteins. These acetylation modifiers are involved in a variety of pathophysiological processes contributing to the development of renal fibrosis, including partial

epithelial-mesenchymal transition, renal fibroblast activation, inflammatory response, and expression of profibrotic factors [50].

In addition, acceleration of COL1A1/COL1A2 collagen expression can be regulated by histone modification under the influence of various physiological and pathological processes [50-53]. Histone modifications stimulate the process of epithelial-mesenchymal transition, which promotes transformation of the epithelium of the nephron tubules into stromal cells. This mechanism causes dysfunction of all parts of the nephron in chronic renal failure [50,53]. Activated myofibroblasts formed during EMT, arising from the epithelium of the nephron, can play a key role in developing kidney fibrosis providing excessive formation of the extracellular matrix [8,54]. Although the most likely mechanism associated with the development of fibrosis is transformation of disrupted tubular epithelial cells into mesenchymal cells, their exact mechanisms have not yet been discovered. Kidney fibrosis is accompanied by an increased content of myofibroblasts, more than a third of which originate from tubular epithelial cells [35,36]. The increased expression of smooth muscle actin, demonstrated in our study, supports the increased number of myofibroblasts at the sites with fibrotic changes and the high intensity of the epithelial-mesenchymal transition. Similar situations are known in other organs, for example, the lungs [55].

The results obtained indirectly support the involvement of specific mast cell proteases in the epithelial-mesenchymal process. Indeed, as well known, the nuclear histone state is regulated epigenetically by tryptase [56-58]. EMT is likely to be implemented due to tryptase action, the fact that has not previously been evidenced in the available resources. A study of the fundamental importance of tryptase transport into cell nuclei stated the ability of the protease to process core histones in the N-terminal tail and change transcription processes [56-58]. Notably, the enzymatic tryptase activity in the nucleus is stabilized by DNA molecules, thus potentiating long-term regulation of the state of histones [56,58,59]. This principle of regulation of core histone epigenetic modifications is a specific function of human mast cell tryptase [58]. Close colocalization of CPA3 with tryptase, which we have identified in our studies (unpublished findings), creates prerequisites for carboxypeptidase A3 participation in particular epigenetic effects [24].

The results of our research study have demonstrated formation of certain areas of cells containing tryptase; the fact supporting potential mechanisms for protease participation in epithelial-mesenchymal transformation. Concurrently, the undulating-like process affects a limited number of cells at the first stages; they are likely to become active cellular foci of increased synthesis of extracellular matrix components in the following.

Strong evidence for carboxypeptidase A3 participation in the regulation of fibrous niches suggests unknown mechanisms. Based on the known facts about the manifestation of the biological effects of CPA3 in cooperation with chymase, one can also assume the importance of this protease in the progression of fibrotic changes. Thus, the results of the performed analysis emphasize the role of mast cells in the formation of fibrotic changes in the kidneys. The identified potential to develop a pro-inflammatory profile of a specific tissue microenvironment and provide epigenetic modification of histones using tryptase invents a new mechanism of the kidney tubulointerstitial fibrosis progression, which has both important diagnostic criteria and allows determining future pharmacological targets for the prevention and treatment of the disease. The formation of local areas of the stroma with a high content of tryptase, in its essence, should be limited by additional structural elements that regulate the diffusion rate and their final concentration in a strictly limited tissue volume. This regulation can be assumably performed by telocytes, which have a significant function in the organization and regulation of the stroma of the kidneys [60,61]; however, this issue requires further detail analysis.

4. Materials and methods

4.1. Case report

The study involved biomaterial of the kidney obtained from a 3-year-old patient after heminephroureterotomy of the upper pole of the duplex right kidney performed at Veltishev

Research and Clinical Institute for Pediatrics & Pediatric Surgery of the Pirogov Russian National Research Medical University of the Russian Ministry of Health (hereafter - Veltischev Institute).

Clinical history provided information on the presenting complaints, past medical and social history etc. The patient was a child born in the 3rd pregnancy. The pregnancy was accompanied by severe polyhydramnios; a single tight loop of cord was present around the neck of the fetus. The baby was born at due time, at the 40th week of gestation. After birth, the baby was diagnosed with a congenital malformation of the urinary system organs: incomplete duplication of the right kidney, hydronephrotic transformation of the ventral part of the duplex kidney, cervical ectopia, stenosis and ureterocele of the ureteral orifice of the upper pole of the duplex right kidney. At the age of 3 months, the baby underwent endoscopic dissection of the ureterocele on the right due to obstructive hydronephrosis, the procedure was performed at the local medical facilities. At 19 and 32 months, there were repeated interventions to perform endoscopic correction of the ureteral orifice of the upper pole of the duplex right kidney, which resulted in the formation of vesicoureteral reflux of the 4th degree complicated by the development of recurrent obstructive pyelonephritis. Computed tomography with contrast, performed during examination at Veltischev Institute, revealed an incomplete doubling of the right kidney, hydronephrosis of the upper pole of the right kidney the 4th degree with signs of the parenchyma atrophy. According to static nephroscintigraphy, the integral capture index of the upper pole of the right kidney was 7%. Due to non-functioning upper pole of the duplex right kidney, signs of nephrosclerosis, presence of recurrent pyelonephritis, there was made a decision to perform heminefroureterotomy of the upper pole of the duplex right kidney.

This study was conducted in accordance with the World Medical Association Declaration of Helsinki "Ethical Principles for Medical Research Involving Human Subjects" and approved by the local ethical committee of Veltischev Institute. Informed consent was obtained from the legal representative of the child. Samples were de-identified.

4.2. Tissue Probe Staining

Tissue probes left over during the routine diagnostic procedure were fixed in buffered 4% formaldehyde and routinely embedded in paraffin. Paraffin tissue sections (5 and 2 μm thick for histochemical and immunohistochemical staining, respectively) were deparaffinized with xylene and rehydrated with graded ethanols according to a standard procedure [19].

4.3. Immunohistochemistry and histochemistry

For the immunohistochemical assay, we subjected deparaffinized sections to antigen retrieval by heating the sections in a steamer with R-UNIVERSAL Epitope Recovery Buffer (Aptum Biologics Ltd., Southampton, SO16 8AD, UK), at 95 °C × 30 min. Blocking the endogenous Fc receptors prior to incubation with primary antibodies was omitted, according to our earlier recommendations [20]. After antigen retrieval and, when required, quenching endogenous peroxidase, sections were immunoreacted with primary antibodies. The list of primary antibodies used in this study is presented in Table 5. Immunohistochemical visualization of bound primary antibodies was performed either with Ventana Slide Stainer or manually, according to the standard protocol [20]. For manually performed immunostaining, primary antibodies were applied in concentration from 1 to 5 μg/mL and incubated overnight at +4 °C.

Table 5. Primary antibodies used in this study.

Antibodies	Host	Catalogue Nr.	Dilution	Source
Tryptase	Mouse monoclonal Ab	#ab2378	1:3000	AbCam, United Kingdom
Tryptase	Rabbit monoclonal [EPR9522]	#ab151757	1:1000	AbCam, United Kingdom

Carboxypeptidase A3 (CPA3)	Rabbit polyclonal Ab	#ab251696	1:2000	AbCam, United Kingdom
Chymase	Mouse monoclonal Ab[CC1]	ab2377	1:2000	AbCam, United Kingdom
α SMA	Mouse monoclonal [1A4]	ab7817	1:2000	AbCam, United Kingdom
Vimentin	Rabbit monoclonal [EPR3776]	ab92547	1:1000	AbCam, United Kingdom

Bound primary antibodies were visualized using secondary antibodies (purchased from Dianova, Hamburg, Germany, and Molecular Probes, Darmstadt, Germany) conjugated with Alexa Fluor-488 or Cy3. The final concentration of secondary antibodies was between 5 and 10 μ g/mL PBS. Single and multiple immunofluorescence labeling were performed according to standard protocols [19]. The list of secondary antibodies and other reagents used in this study is presented in Table 6.

Histochemical staining with Toluidine blue, May Grünwald, Giemsa and picro-Mallory solutions, Heidenhain’s azan trichrome, alcian blue, Mayer’s hematoxylin and eosin, and silver impregnation were performed according to the manufacturer’s instructions (Table 7).

Table 6. Secondary antibodies and other reagents.

	Source	Dilution	Label
Goat anti-mouse IgG Ab (#ab97035)	AbCam, United Kingdom	1/500	Cy3
Goat anti-rabbit IgG Ab (#ab150077):	AbCam, United Kingdom	1/500	Alexa Fluor 488
AmpliStain™ anti-Mouse 1-Step HRP (#AS-M1-HRP)	SDT GmbH, Baesweiler, Germany	ready-to-use	HRP
AmpliStain™ anti-Rabbit 1-Step HRP (#AS-R1-HRP)	SDT GmbH, Baesweiler, Germany	ready-to-use	HRP
4',6-diamidino-2-phenylindole (DAPI, #D9542-5MG)	Sigma, Hamburg, Germany	5 μ g/mL	w/o
VECTASHIELD® Mounting Medium (#H-1000)	Vector Laboratories, Burlingame, CA, USA	ready-to-use	w/o
DAB Peroxidase Substrat Kit (#SK-4100)	Vector Laboratories, Burlingame, CA, USA	ready-to-use	DAB

Table 7. Reagents used for histochemical staining.

Dyes	Catalogue Number	Provider	Dilution	Manufacturer
Toluidine blue	07-002	Biovitrum	Ready-to-use	ErgoProduction LLC, Russia
Giemsa solution	20-043/L	Biovitrum	Ready-to-use	ErgoProduction LLC, Russia
Silver impregnation	21-026	Biovitrum	Ready-to-use	ErgoProduction LLC, Russia
Mayer’s hematoxylin	HK-G0-DL01	Biovitrum	Ready-to-use	ErgoProduction LLC, Russia
Picro Mallori trichrome	21-036	Biovitrum	Ready-to-use	ErgoProduction LLC, Russia
Heidenhain’s Azan trichrome	21-041	Biovitrum	Ready-to-use	ErgoProduction LLC, Russia
Giemsa	20-023	Biovitrum	Ready-to-use	ErgoProduction LLC, Russia
May-Grunwald-Giemsa	21-068	Biovitrum	Ready-to-use	ErgoProduction LLC, Russia
Alcian blue pH 2.5	21-069/L	Biovitrum	Ready-to-use	ErgoProduction LLC, Russia
Eosin Y 1% aqueous	HK-EV-A250	Biovitrum	Ready-to-use	ErgoProduction LLC, Russia

4.4. Controls

Control incubations were: omission of primary antibodies or substitution of primary antibodies by the same IgG species (Dianova, Hamburg, Germany) at the same final concentration as the primary antibodies. The exclusion of either the primary or the secondary antibody from the immunohistochemical reaction and the substitution of primary antibodies with the corresponding IgG at the same final concentration resulted in a lack of immunostaining. The specific and selective staining of different cells with the use of primary antibodies from the same species on the same preparation is, by itself, sufficient control for the immunostaining specificity.

4.5. Image Acquisition

Stained tissue sections were observed on a ZEISS Axio Imager.Z2 equipped with a Zeiss alpha Plan-Apochromat objective 100×/1.46 Oil DIC M27, a Zeiss Objective Plan-Apochromat 150×/1.35 Glyc DIC Corr M27 and a ZEISS Axiocam 712 color digital microscope camera. Captured images were processed with the software program “Zen 3.0 Light Microscopy Software Package”, “ZEN Module Bundle Intellesis & Analysis for Light Microscopy”, “ZEN Module Z Stack Hardware” (Carl Zeiss Vision, Jena, Germany) and submitted with the final revision of the manuscript at 300 DPI. Photomicrographs were obtained in some cases with Nikon D-Eclipse C1 Si confocal microscope based on Nikon Eclipse 90i.

4.6. Quantitative analysis

A nephrofibrotic kidney was dissected into 4 fragments to increase the volume of analyzed structural components, quantitative data and, accordingly, objectivity of the findings received. Sections were prepared from each fragment and stained by immunohistochemical methods in accordance with Section 3.3. Planimetric analysis to determine the number of MCs per a unit area of the kidney tissue, as well as the absolute number of MCs and other kidney cells, was determined using open-source software for digital pathology image analysis QuPath [21]. Morphometric analysis to identify the area of immunopositive structures on SMA and vimentin in relation to the total size of the kidney tissues on histological sections, and to determine the absolute number of tryptase-positive nuclei in relation to the total number of nuclei on sections was carried out using software QuPath [21] with further calculation of the relative content (Table 1). The cortex and medulla of the kidney, as well as parts of the organ with pronounced manifestations of fibrotic changes, were analyzed separately. When determining SMA- and Vimentin-positive cells and structures, kidney vessels were excluded from the analyzed areas to objectify the data obtained. To obtain the integral values of the studied parameters of mast cells and fibrosis, the average value was obtained from the results of the analysis of each kidney fragment.

4.7. Data Availability

The authors declare that all the data supporting the findings of this work are available within the article or from the corresponding author upon reasonable request.

5. Conclusions

The results obtained evidence that, along with pronounced fibrotic changes in the pathogenic kidney, a multilocular process is present and new profibrogenic niches are formed with active mast cell participation through tryptase, chymase, and carboxypeptidase A3 secretion. Mast cells are able to develop inducing effects of the local tissue microenvironment on fibroblast activation, inflammation, epithelial-mesenchymal transition activity, and vascular homeostasis in profibrogenic niches. Identification of the molecular biological parameters of mast cells, primarily those associated with inflammatory loci, is an innovative approach to identify the fundamental mechanisms of nephrofibrosis. The biological relevance of mast cells in the formation of fibrogenic niches can be used not only to make timely and correct diagnosis and administer an effective therapy, but also to prevent tubulointerstitial fibrosis of various etiologies.

Author Contributions: All authors were actively involved with the work on this manuscript. D.A. and S.M. designed the study, M.I. and G.K. performed experiments, S.B., V.D. and I.B. analyzed the received data, D.A. and S.M. carried out microphotographs and wrote the manuscript, V.D. and M.T. supervised the study. All authors have read and agreed to the published version of the manuscript.

Funding Statement: This research received no external funding.

Institutional Review Board Statement: This study was conducted in accordance with the World Medical Association Declaration of Helsinki "Ethical Principles for Medical Research Involving Human Subjects" and approved by the local ethical committee of Veltischev Research and Clinical Institute for Pediatrics & Pediatric Surgery of the Pirogov Russian National Research Medical University of the Russian Ministry of Health (approval protocol No.4, 10 March 2023).

Informed Consent Statement: The samples were retrieved from the Veltischev Research and Clinical Institute for Pediatrics & Pediatric Surgery (Moscow, Russia). Informed consent was obtained from subject. The sample was qualified as redundant clinical specimen that had been de-identified and unlinked from patient information.

Data Availability Statement: All data and materials are available on reasonable request. Address to D.A. (email: atyakshin-da@rudn.ru) or S.M. (email: mser@list.ru).

Conflicts of Interest: The authors declare no competing interest.

Acknowledgments: This publication has been supported by RUDN University project № 210500-2-000, «Molecular mechanisms of mast cell participation in the formation of the immune and stromal landscape of a specific tissue microenvironment in normal and pathological conditions».

References

1. Collaboration, G.B.D.C.K.D. Global, regional, and national burden of chronic kidney disease, 1990-2017: a systematic analysis for the Global Burden of Disease Study 2017. *Lancet* **2020**, *395*, 709-733, doi:10.1016/S0140-6736(20)30045-3.
2. Chen, T.K.; Knicely, D.H.; Grams, M.E. Chronic Kidney Disease Diagnosis and Management: A Review. *JAMA* **2019**, *322*, 1294-1304, doi:10.1001/jama.2019.14745.
3. Ruiz-Ortega, M.; Rayego-Mateos, S.; Lamas, S.; Ortiz, A.; Rodrigues-Diez, R.R. Targeting the progression of chronic kidney disease. *Nat Rev Nephrol* **2020**, *16*, 269-288, doi:10.1038/s41581-019-0248-y.
4. Li, L.; Fu, H.; Liu, Y. The fibrogenic niche in kidney fibrosis: components and mechanisms. *Nat Rev Nephrol* **2022**, *18*, 545-557, doi:10.1038/s41581-022-00590-z.
5. Edeling, M.; Ragi, G.; Huang, S.; Pavenstadt, H.; Susztak, K. Developmental signalling pathways in renal fibrosis: the roles of Notch, Wnt and Hedgehog. *Nat Rev Nephrol* **2016**, *12*, 426-439, doi:10.1038/nrneph.2016.54.
6. Bulow, R.D.; Boor, P. Extracellular Matrix in Kidney Fibrosis: More Than Just a Scaffold. *J Histochem Cytochem* **2019**, *67*, 643-661, doi:10.1369/0022155419849388.
7. Sato, Y.; Yanagita, M. Resident fibroblasts in the kidney: a major driver of fibrosis and inflammation. *Inflamm Regen* **2017**, *37*, 17, doi:10.1186/s41232-017-0048-3.
8. Wei, J.; Xu, Z.; Yan, X. The role of the macrophage-to-myofibroblast transition in renal fibrosis. *Front Immunol* **2022**, *13*, 934377, doi:10.3389/fimmu.2022.934377.
9. Chen, P.S.; Li, Y.P.; Ni, H.F. Morphology and Evaluation of Renal Fibrosis. *Adv Exp Med Biol* **2019**, *1165*, 17-36, doi:10.1007/978-981-13-8871-2_2.
10. Theoharides, T.C. Neuroendocrinology of mast cells: Challenges and controversies. *Exp Dermatol* **2017**, *26*, 751-759, doi:10.1111/exd.13288.
11. Elieh Ali Komi, D.; Wohrl, S.; Bielory, L. Mast Cell Biology at Molecular Level: a Comprehensive Review. *Clin Rev Allergy Immunol* **2020**, *58*, 342-365, doi:10.1007/s12016-019-08769-2.
12. Valent, P.; Akin, C.; Hartmann, K.; Nilsson, G.; Reiter, A.; Hermine, O.; Sotlar, K.; Sperr, W.R.; Escribano, L.; George, T.I.; et al. Mast cells as a unique hematopoietic lineage and cell system: From Paul Ehrlich's visions to precision medicine concepts. *Theranostics* **2020**, *10*, 10743-10768, doi:10.7150/thno.46719.

13. Galli, S.J.; Gaudenzio, N.; Tsai, M. Mast Cells in Inflammation and Disease: Recent Progress and Ongoing Concerns. *Annu Rev Immunol* **2020**, *38*, 49-77, doi:10.1146/annurev-immunol-071719-094903.
14. Komi, D.E.A.; Redegeld, F.A. Role of Mast Cells in Shaping the Tumor Microenvironment. *Clin Rev Allergy Immunol* **2020**, *58*, 313-325, doi:10.1007/s12016-019-08753-w.
15. Kolkhir, P.; Elieh-Ali-Komi, D.; Metz, M.; Siebenhaar, F.; Maurer, M. Understanding human mast cells: lesson from therapies for allergic and non-allergic diseases. *Nat Rev Immunol* **2022**, *22*, 294-308, doi:10.1038/s41577-021-00622-y.
16. Owens, E.P.; Vesey, D.A.; Kassianos, A.J.; Healy, H.; Hoy, W.E.; Gobe, G.C. Biomarkers and the role of mast cells as facilitators of inflammation and fibrosis in chronic kidney disease. *Transl Androl Urol* **2019**, *8*, S175-S183, doi:10.21037/tau.2018.11.03.
17. Atiakshin, D.; Buchwalow, I.; Tiemann, M. Mast cells and collagen fibrillogenesis. *Histochem Cell Biol* **2020**, *154*, 21-40, doi:10.1007/s00418-020-01875-9.
18. Zhou, Y.; Wei, M.; Zhang, M.; Zhang, J.; Tang, F.; Wu, X. Adefovir accumulation in the renal interstitium triggers mast cell degranulation and promotes renal interstitial fibrosis. *Toxicol Lett* **2022**, *359*, 10-21, doi:10.1016/j.toxlet.2022.01.018.
19. Buchwalow, I.B.; Böcker, W. *Immunohistochemistry: basics and methods*; Springer Science & Business Media: 2010.
20. Buchwalow, I.; Samoilova, V.; Boecker, W.; Tiemann, M. Non-specific binding of antibodies in immunohistochemistry: fallacies and facts. *Sci Rep* **2011**, *1*, 28, doi:10.1038/srep00028.
21. Bankhead, P.; Loughrey, M.B.; Fernandez, J.A.; Dombrowski, Y.; McArt, D.G.; Dunne, P.D.; McQuaid, S.; Gray, R.T.; Murray, L.J.; Coleman, H.G.; et al. QuPath: Open source software for digital pathology image analysis. *Sci Rep* **2017**, *7*, 16878, doi:10.1038/s41598-017-17204-5.
22. Atiakshin, D.; Buchwalow, I.; Samoilova, V.; Tiemann, M. Tryptase as a polyfunctional component of mast cells. *Histochem Cell Biol* **2018**, *149*, 461-477, doi:10.1007/s00418-018-1659-8.
23. Atiakshin, D.; Buchwalow, I.; Tiemann, M. Mast cell chymase: morphofunctional characteristics. *Histochem Cell Biol* **2019**, *152*, 253-269, doi:10.1007/s00418-019-01803-6.
24. Atiakshin, D.; Kostin, A.; Trotsenko, I.; Samoilova, V.; Buchwalow, I.; Tiemann, M. Carboxypeptidase A3-A Key Component of the Protease Phenotype of Mast Cells. *Cells* **2022**, *11*, doi:10.3390/cells11030570.
25. Fu, H.; Tian, Y.; Zhou, L.; Zhou, D.; Tan, R.J.; Stolz, D.B.; Liu, Y. Tenascin-C Is a Major Component of the Fibrogenic Niche in Kidney Fibrosis. *J Am Soc Nephrol* **2017**, *28*, 785-801, doi:10.1681/ASN.2016020165.
26. Theoharides, T.C.; Alysandratos, K.D.; Angelidou, A.; Delivanis, D.A.; Sismanopoulos, N.; Zhang, B.; Asadi, S.; Vasiadi, M.; Weng, Z.; Miniati, A.; et al. Mast cells and inflammation. *Biochim Biophys Acta* **2012**, *1822*, 21-33, doi:10.1016/j.bbdis.2010.12.014.
27. Gonzalez-de-Olano, D.; Alvarez-Twose, I. Mast Cells as Key Players in Allergy and Inflammation. *J Investig Allergol Clin Immunol* **2018**, *28*, 365-378, doi:10.18176/jiaci.0327.
28. Zhang, Z.; Kurashima, Y. Two Sides of the Coin: Mast Cells as a Key Regulator of Allergy and Acute/Chronic Inflammation. *Cells* **2021**, *10*, doi:10.3390/cells10071615.
29. Hughes, M.R.; McNagny, K.M. Preface. Mast cells. *Methods Mol Biol* **2015**, *1220*, vii-viii, doi:10.1007/978-1-4939-1568-2.
30. O'Connell, M.P.; Lyons, J.J. Resolving the genetics of human tryptases: implications for health, disease, and clinical use as a biomarker. *Curr Opin Allergy Clin Immunol* **2022**, *22*, 143-152, doi:10.1097/ACI.0000000000000813.
31. Hellman, L.; Akula, S.; Fu, Z.; Wernersson, S. Mast Cell and Basophil Granule Proteases - In Vivo Targets and Function. *Front Immunol* **2022**, *13*, 918305, doi:10.3389/fimmu.2022.918305.
32. Vitte, J. Human mast cell tryptase in biology and medicine. *Mol Immunol* **2015**, *63*, 18-24, doi:10.1016/j.molimm.2014.04.001.
33. Longo, V.; Tamma, R.; Brunetti, O.; Pisconti, S.; Argentiero, A.; Silvestris, N.; Ribatti, D. Mast cells and angiogenesis in pancreatic ductal adenocarcinoma. *Clin Exp Med* **2018**, *18*, 319-323, doi:10.1007/s10238-018-0493-6.
34. Pejler, G.; Abrink, M.; Ringvall, M.; Wernersson, S. Mast cell proteases. *Adv Immunol* **2007**, *95*, 167-255, doi:10.1016/S0065-2776(07)95006-3.
35. Iwano, M.; Plieth, D.; Danoff, T.M.; Xue, C.; Okada, H.; Neilson, E.G. Evidence that fibroblasts derive from epithelium during tissue fibrosis. *J Clin Invest* **2002**, *110*, 341-350, doi:10.1172/JCI15518.
36. Ribatti, D.; Tamma, R. Giulio Gabbiani and the discovery of myofibroblasts. *Inflamm Res* **2019**, *68*, 241-245, doi:10.1007/s00011-018-01211-x.
37. Chimenti, M.S.; Sunzini, F.; Fiorucci, L.; Botti, E.; Fonti, G.L.; Conigliaro, P.; Triggianese, P.; Costa, L.; Caso, F.; Giunta, A.; et al. Potential Role of Cytochrome c and Tryptase in Psoriasis and Psoriatic Arthritis Pathogenesis: Focus on Resistance to Apoptosis and Oxidative Stress. *Front Immunol* **2018**, *9*, 2363, doi:10.3389/fimmu.2018.02363.
38. Lucena, F.; McDougall, J.J. Protease Activated Receptors and Arthritis. *Int J Mol Sci* **2021**, *22*, doi:10.3390/ijms22179352.

39. Pejler, G. Novel Insight into the in vivo Function of Mast Cell Chymase: Lessons from Knockouts and Inhibitors. *J Innate Immun* **2020**, *12*, 357-372, doi:10.1159/000506985.
40. He, S.; Walls, A.F. Human mast cell chymase induces the accumulation of neutrophils, eosinophils and other inflammatory cells in vivo. *Br J Pharmacol* **1998**, *125*, 1491-1500, doi:10.1038/sj.bjp.0702223.
41. Takato, H.; Yasui, M.; Ichikawa, Y.; Waseda, Y.; Inuzuka, K.; Nishizawa, Y.; Tagami, A.; Fujimura, M.; Nakao, S. The specific chymase inhibitor TY-51469 suppresses the accumulation of neutrophils in the lung and reduces silica-induced pulmonary fibrosis in mice. *Exp Lung Res* **2011**, *37*, 101-108, doi:10.3109/01902148.2010.520815.
42. Takai, S.; Jin, D. Pathophysiological Role of Chymase-Activated Matrix Metalloproteinase-9. *Biomedicines* **2022**, *10*, doi:10.3390/biomedicines10102499.
43. Vibhushan, S.; Bratti, M.; Montero-Hernandez, J.E.; El Ghoneimi, A.; Benhamou, M.; Charles, N.; Daugas, E.; Blank, U. Mast Cell Chymase and Kidney Disease. *Int J Mol Sci* **2020**, *22*, doi:10.3390/ijms22010302.
44. Lin, L.; Bankaitis, E.; Heimbach, L.; Li, N.; Abrink, M.; Pejler, G.; An, L.; Diaz, L.A.; Werb, Z.; Liu, Z. Dual targets for mouse mast cell protease-4 in mediating tissue damage in experimental bullous pemphigoid. *J Biol Chem* **2011**, *286*, 37358-37367, doi:10.1074/jbc.M111.272401.
45. Dell'Italia, L.J.; Collawn, J.F.; Ferrario, C.M. Multifunctional Role of Chymase in Acute and Chronic Tissue Injury and Remodeling. *Circ Res* **2018**, *122*, 319-336, doi:10.1161/CIRCRESAHA.117.310978.
46. Akula, S.; Hellman, L.; Aviles, F.X.; Wernersson, S. Analysis of the mast cell expressed carboxypeptidase A3 and its structural and evolutionary relationship to other vertebrate carboxypeptidases. *Dev Comp Immunol* **2022**, *127*, 104273, doi:10.1016/j.dci.2021.104273.
47. Atiakshin, D.; Kostin, A.; Trotsenko, I.; Shishkina, V.; Tiemann, M.; Buchwalow, I. Carboxypeptidase A3 in the structure of the protease phenotype of mast cells: cytophysiological aspects. *RUDN Journal of Medicine* **2022**, *26(1)*, 9-33, doi:10.22363/2313-0245-2022-26-1-9-33.
48. Bonasio, R.; Tu, S.; Reinberg, D. Molecular signals of epigenetic states. *Science* **2010**, *330*, 612-616, doi:10.1126/science.1191078.
49. Sun, J.; Wang, Y.; Cui, W.; Lou, Y.; Sun, G.; Zhang, D.; Miao, L. Role of Epigenetic Histone Modifications in Diabetic Kidney Disease Involving Renal Fibrosis. *J Diabetes Res* **2017**, *2017*, 7242384, doi:10.1155/2017/7242384.
50. Shen, F.; Zhuang, S. Histone Acetylation and Modifiers in Renal Fibrosis. *Front Pharmacol* **2022**, *13*, 760308, doi:10.3389/fphar.2022.760308.
51. Thomas, M.C. Epigenetic Mechanisms in Diabetic Kidney Disease. *Curr Diab Rep* **2016**, *16*, 31, doi:10.1007/s11892-016-0723-9.
52. Yuan, H.; Reddy, M.A.; Deshpande, S.; Jia, Y.; Park, J.T.; Lanting, L.L.; Jin, W.; Kato, M.; Xu, Z.G.; Das, S.; et al. Epigenetic Histone Modifications Involved in Profibrotic Gene Regulation by 12/15-Lipoxygenase and Its Oxidized Lipid Products in Diabetic Nephropathy. *Antioxid Redox Signal* **2016**, *24*, 361-375, doi:10.1089/ars.2015.6372.
53. Wang, J.; Li, J.; Zhang, X.; Zhang, M.; Hu, X.; Yin, H. Molecular mechanisms of histone deacetylases and inhibitors in renal fibrosis progression. *Front Mol Biosci* **2022**, *9*, 986405, doi:10.3389/fmolb.2022.986405.
54. Yuan, Q.; Tan, R.J.; Liu, Y. Myofibroblast in Kidney Fibrosis: Origin, Activation, and Regulation. *Adv Exp Med Biol* **2019**, *1165*, 253-283, doi:10.1007/978-981-13-8871-2_12.
55. Kondratyuk, R.; Grekov, I.; Seleznev, E. Microenvironment influence on the development of epithelial-mesenchymal transformation in lung cancer. *RUDN Journal of MEDICINE* **2022**, *26(3)*, 325-337, doi:10.22363/2313-0245-2022-26-3-325-337.
56. Melo, F.R.; Vita, F.; Berent-Maoz, B.; Levi-Schaffer, F.; Zabucchi, G.; Pejler, G. Proteolytic histone modification by mast cell tryptase, a serglycin proteoglycan-dependent secretory granule protease. *J Biol Chem* **2014**, *289*, 7682-7690, doi:10.1074/jbc.M113.546895.
57. Rabelo Melo, F.; Santosh Martin, S.; Sommerhoff, C.P.; Pejler, G. Exosome-mediated uptake of mast cell tryptase into the nucleus of melanoma cells: a novel axis for regulating tumor cell proliferation and gene expression. *Cell Death Dis* **2019**, *10*, 659, doi:10.1038/s41419-019-1879-4.
58. Alanazi, S.; Rabelo Melo, F.; Pejler, G. Tryptase Regulates the Epigenetic Modification of Core Histones in Mast Cell Leukemia Cells. *Front Immunol* **2021**, *12*, 804408, doi:10.3389/fimmu.2021.804408.
59. Alanazi, S.; Grujic, M.; Lampinen, M.; Rollman, O.; Sommerhoff, C.P.; Pejler, G.; Melo, F.R. Mast Cell beta-Tryptase Is Enzymatically Stabilized by DNA. *Int J Mol Sci* **2020**, *21*, doi:10.3390/ijms21145065.
60. Wolnicki, M.; Aleksandrovych, V.; Gil, K. Interstitial cells of Cajal and telocytes in the urinary system: facts and distribution. *Folia Med Cracov* **2016**, *56*, 81-89.
61. Sanches, B.D.A.; Tamarindo, G.H.; Maldarine, J.D.S.; Da Silva, A.D.T.; Dos Santos, V.A.; Goes, R.M.; Taboga, S.R.; Carvalho, H.F. Telocytes of the male urogenital system: Interrelationships, possible functions, and pathological implications. *Cell Biol Int* **2021**, *45*, 1613-1623, doi:10.1002/cbin.11612.